PHYSICAL REVIEW D VOLUME 27, NUMBER 5 1 MARCH 1983

Spectator-based pole model for three-body nonleptonic decays of D and F mesons

Robert D. C. Miller
Theoretical Physics Group, School of Physics, University of Melbourne, Parkville, Victoria, 3052, Australia

Bruce H. J. McKellar
Theoretical Physics Group, School of Physics, University of Melbourne, Parkville, Victoria, 3052, Australia and Theoretical Division, Los Alamos National Laboratory, Los Alamos, New Mexico 87545*

(Received 10 May 1982; revised manuscript received 30 June 1982)

The spectator model of charmed-particle decays has failed to reproduce the two-body decay data. Soft-pion/kaon arguments have led to the belief that it is equally condemned to fail for three-body decays. However, avoiding soft-pion/kaon analyses we are led to a pole model of three-body decay which is in good agreement with the branching-ratio data, and the observed $\tau(D^+)/\tau(D^0)$ ratio.

I. INTRODUCTION

One of the earliest, simplest, and most appealing models of charmed-meson decays is the spectator model[1] in which the charmed quark is assumed to decay, and the other constituent quark of the meson behaves as an independent spectator, as in Fig. 1(A). Two of the predictions of this model

$$\text{(i)}\quad \tau(D^+)=\tau(D^0)\,,$$

$$\text{(ii)}\quad \frac{\Gamma(D^0\to\bar{K}^0\pi^0)}{\Gamma(D^0\to K^-\pi^+)}\approx 0.025$$

are in marked disagreement with the experimental data[2]

$$\text{(i')}\quad \tau(D^+)/\tau(D^0)=3.1^{+4.6}_{-1.4}\,,$$

$$\text{(ii')}\quad \frac{\Gamma(D^0\to\bar{K}^0\pi^0)}{\Gamma(D^0\to K^-\pi^+)}=0.75\pm 0.34\,.$$

This disagreement has prompted many modifications of the spectator model, which may be reviewed in Leveille[3] and Pakvasa.[4] These include: (a) dominance of nonspectator graphs,[5] (b) inclusion of perturbative gluon effects,[6] (c) inclusion of nonperturbative gluon effects,[7,8] (d) phenomenological modification of the spectator model,[9] (e) inclusion of final-state interactions,[10,11] and (f) even more exotic possibilities,[12] in part generated by further difficulties in understanding the Cabibbo-suppressed decays. However none of these modifications are totally convincing, and their number indicates that we are a long way from understanding the two-body decays of the charmed mesons.

Partly because of these difficulties with the description of what one would expect to be the simplest charmed-meson decays, very little work has been done on the three-body decay modes.[13–17] In particular from soft-pion and soft-kaon theorems one would expect to relate the $K2\pi$ modes to the $K\pi$ modes—which is not much encouragement to proceed when the $K\pi$ modes are not well understood.

Nevertheless in this paper we adapt the simple spectator model to attempt a description of the three-body decay modes. We are undeterred by the

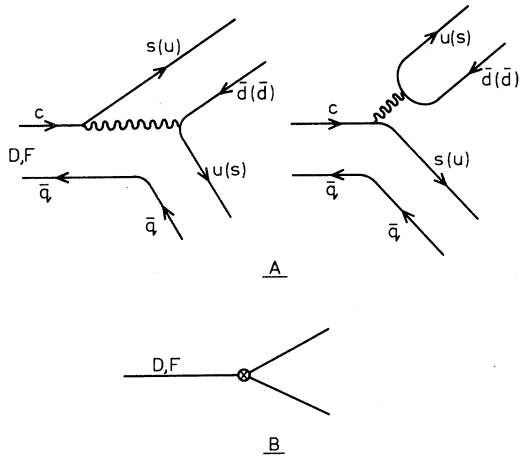

FIG. 1. (A) Spectator diagrams of charm decay permitted by Eq. (3). As usual the four-body weak vertex is drawn so as to indicate color flow. (B) Macroscopic view of spectator diagrams. ⊗ represents the weak vertex.

failure of the model for the two-body modes, noting that two-body modes are parity violating, and the three-body modes are parity conserving. A successful simultaneous understanding of parity-violating and parity-conserving strange-particle decays proved elusive for many years,[18,19] and not everybody is convinced that the problem is yet solved.[4] Moreover, sufficient structure is observed in the Dalitz plot of the three-body decays[2] that one would not expect the soft-pion and soft-kaon results to give a good description of the overall three-body rate. And furthermore it has been suggested that the spectator model need not necessarily lead to the equality of D^+ and D^0 lifetimes.[20] For all of these reasons it is desirable to approach the study of the three-body decay modes free of inhibitions generated by the study of the two-body decays.

We develop a simple pole model of the three-body decays, in which the basic charm-changing weak process is the parity-conserving decay $P_c \to VP$ or $P_c \to SP$ of the charmed pseudoscalar meson P_c to uncharmed vector and pseudoscalar or scalar and pseudoscalar. Subsequent decay of the vector or scalar meson produces the three-pseudoscalar final state. The pole graphs representing our model are shown in Fig. 2. We should emphasize that, although Sezgin[15] has considered a few of the dominant three-body decay modes in a pole model, his pole model differs essentially from ours.

In Sec. II we will show how the spectator model for $P_c \to VP$ and $P_c \to SP$ implicates our pole model, dominated by uncharmed vector- and scalar-meson poles. Our model has two free parameters, the absolute magnitude of the weak interaction and the relative strength of scalar and vector terms. In view of the well known difficulties in calculating the two-body modes, we have

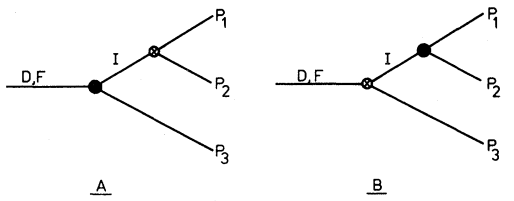

FIG. 2. The spectator-derived pole model of three-body decays of charmed mesons. Either the strong vertex (●) occurs before the weak vertex (⊗) leading to a charmed-meson pole (case A), or the weak vertex occurs before the strong leading to a noncharmed meson pole (case B).

confined ourselves to calculating ratios of three-body rates, eliminating one of the parameters. It then turns out that the branching ratios observed at present are insensitive to the relative strength of the vector and scalar poles and are reasonably well described by our model. Certain F decay modes and some kinematically suppressed D decay modes are sensitive to the strength of the scalar pole, and could be used to measure this parameter. Our model is also consistent with present data on the lifetimes of D^+ and D^0, which is contrary to one's naive expectations for a spectator model. These results are presented in Sec. III, and we make some concluding remarks in Sec. IV.

II. FROM THE SPECTATOR TO THE POLE MODEL

A. Foundations

We base our work on the same basic QCD-renormalized Hamiltonian as used by Cabibbo and Maiani,[1]

$$\mathcal{H}_{\text{eff}}^{\Delta C=-1}\ (\text{Cabibbo favored}) = \cos^2\theta_C \frac{G}{\sqrt{2}} \left[\frac{f_+ + f_-}{2} (\bar{s}c)_L (\bar{u}d)_L + \frac{f_+ - f_-}{2} (\bar{s}d)_L (\bar{u}c)_L \right] \tag{1}$$

with their choice of parameters $f_+ = 0.68$, $f_- = 2.15$, which is a sufficiently good approximation to the six-quark Hamiltonian for our present purposes.[21] After Fierz rearrangement the parameters which enter the amplitudes are

$$X_+ = \tfrac{1}{3}(2f_+ + f_-) = 1.17\ , \tag{2a}$$

$$X_- = \tfrac{1}{3}(2f_+ - f_-) = -0.26\ . \tag{2b}$$

In comparing the effective Hamiltonian (1) with the data we must somehow face the problem of converting the quark-level Hamiltonian of Eq. (1) into a Hamiltonian that refers to mesons. The spectator graphs of Fig. 1(A) can be viewed macroscopically as providing a basic weak three-body vertex illustrated in Fig. 1(B). On the other hand annihilation and W exchange graphs lead to macroscopic weak two-body vertices. At the mesonic

level we thus regard spectator dominance as implying that three-body weak vertices will dominate over two-body weak vertices.

We make the connection by regarding the standard Cabibbo-Maiani analysis[1] as supplying us with the relative vertex factor, which we will call the CM factor, for the weak three-body vertex. An overall normalization constant, which may depend on the Lorentz-tensor character of the mesons involved, and the momentum dependence, which is determined by the Lorentz-tensor character of the mesons, may be included phenomenologically (the procedure we adopt) or calculated from the quark wave functions.

Given the basic three-body weak vertex, we are led to consider the three-body decays of the charmed mesons as proceeding through the pole graphs of Fig. 2. The two pole terms differ in whether the weak interaction appears first or second, and thus in Fig. 2(A) the intermediate particle is charmed, while in Fig. 2(B) it is uncharmed. Restricting our consideration to three pseudoscalars in the final state, we see that C and Lorentz invariance of the strong vertex restricts the intermediate meson to be a scalar, vector, or tensor.

In principle we should consider a very large number of possible pole diagrams. We reduce the calculation to manageable proportions by the following observations. In Fig. 3 we illustrate the phase space for $D^+ \to K^- \pi^+ \pi^+$. The peaks of the resonance poles will appear as straight lines on this plot, as we have indicated for the $\bar{K}^{*0}$, the κ^0, and the uncharmed tensor resonance. The nearest charmed pole, the D^*, lies outside the allowed phase space and we therefore do not include the

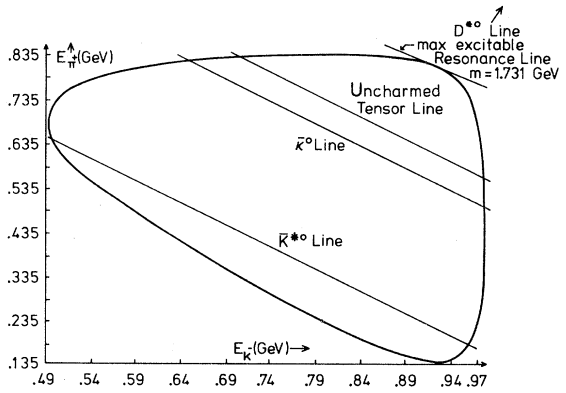

FIG. 3. The kinematically allowed region for $D^+ \to K^- \pi^+ \pi^+$. Resonance poles occur along the lines indicated, as discussed in the text.

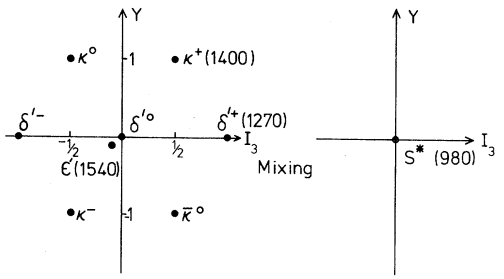

FIG. 4. Our choice of the 0^{++} nonet.

charmed intermediate states in our calculation. We have verified by an explicit calculation that the correction generated by including them is indeed small. Even the uncharmed tensor meson is near the edge of the phase space. For this reason, and because the tensor mesons preferentially couple via the strong interaction to pseudoscalar and vector, rather than two pseudoscalars, we have also neglected tensor meson contributions.

Vector resonances are well inside the phase space and have been observed in the Dalitz plot of the decays, so we must retain them to have a reasonable model. Scalar mesons are also well inside the phase space, are broad, and couple strongly to two pseudoscalars. We therefore also retain them in our model.

In summary, we have argued that the spectator dominance model at the quark level implicates a pole model of charmed-meson decay to three mesons. When the final mesons are three pseudoscalars, the poles of Fig. 2(B) with uncharmed vector and scalar intermediaries will dominate and are retained in our model.

B. Phenomenology

Since we are going to include scalar-meson poles in our model we must make a choice of the 0^{++} scalar nonet. Estabrooks[22] offers two viable alternatives, and we have chosen, the one in which $S^*(980)$ is the mostly SU(3)-singlet member of the 0^{++} nonet (see Fig. 4). The reason for this choice is that it permits an explanation of the coupling ratio $g_{S^*K\bar{K}}/g_{S^*\pi\pi}$ through mixing effects. We recognize that other possible assignments of the $S^*(980)$ as a $qq\bar{q}\bar{q}$ state or as a glueball state have been proposed, but the evidence for these cannot be regarded as convincing.[23] However at least one of the 0^{++} mesons in this mass range must be other than a $q\bar{q}$ state, as there are too many to fit into a

TABLE I. Strong VPP coupling constants $\tilde{g}_{VP_1P_2}$ which enter the pole-model calculation $P_c \to P_1P_2P_3$. The $\tilde{g}_{VP_1P_2}$ are defined in Eq. (4) in the text, and are antisymmetric in P_1 and P_2. Only those coefficients for which $m_2 \geq m_1$ are listed. The others are given by $\tilde{g}_{VP_1P_2} = -\tilde{g}_{VP_2P_1}$.

V	P_1	P_2	$\tilde{g}_{VP_1P_2}$
ρ^+	K^-	K^0	$\sqrt{2}g_{\rho PP}$
ρ^+	π^0	π^-	$2g_{\rho PP}$
ρ^0	π^-	π^+	$2g_{\rho PP}$
ρ^0	K^-	K^+	$g_{\rho PP}$
ρ^0	K^0	$\bar{K}^0$	$g_{\rho PP}$
$\bar{K}^{*0}$	π^-	K^+	$-\sqrt{2}g_{K^*PP}$
$\bar{K}^{*0}$	π^0	K^0	g_{K^*PP}
$\bar{K}^{*0}$	K^0	η^0	$\sqrt{3}g_{K^*PP}$
K^{*-}	π^+	K^0	$-\sqrt{2}g_{K^*PP}$
K^{*-}	π^0	K^+	$-g_{K^*PP}$
K^{*-}	K^+	η^0	$\sqrt{3}g_{K^*PP}$
ϕ^0	K^-	K^+	$\sqrt{2}g_{\phi PP}$
ϕ^0	$\bar{K}^0$	K^0	$\sqrt{2}g_{\phi PP}$

nonet.

With our choice of nonet the quadratic mixing angle for the 0^{++} nonet is given by

$$|\lambda| \approx 22^\circ . \tag{3}$$

We assume ideal mixing for the ω and ϕ, regarding the ϕ as a pure $s\bar{s}$ state, whereas we assume that the η and η' are pure SU(3) octet and singlet, respectively. Small deviations from this assumption do not alter our results significantly.

The phenomenology of the strong-interaction vertices is straightforward. C invariance, SU(3) invariance, and Hermiticity show that the strong vector-pseudoscalar-pseudoscalar vertex may be written as

$$\mathscr{H}^{(s)}_{VPP} = i\tilde{g}_{VP_1P_2} V^\mu P_1 \overleftrightarrow{\partial}_\mu P_2 . \tag{4}$$

$\tilde{g}_{VP_1P_2}$ are real dimensionless coupling constants which contain Clebsch-Gordan coefficients and the ω-ϕ (ideal) mixing angle. They are antisymmetric in P_1 and P_2. $\tilde{g}_{VP_1P_2}$ may be related to a single flavor-SU(3)-invariant coupling g_{VPP}. This is essentially what is done in Table I. However we account for SU(3) breaking by using the experimental values of g_{V_aPP} ($V_a = K^*, \rho, \phi$) obtained from full-width data (see Table II).[24] The approximation thus reduces to one of exact SU(2) rather than SU(3) flavor symmetry.

TABLE II. Numerical values of g_{VPP} coupling constants used in our calculations.

V	g_{VPP}	Source
ρ	3.05	experimental
K^*	3.22	experimental
ϕ	3.26	experimental

Constructing $\mathscr{H}^{(s)}_{SPP}$ in a similar way we find

$$\mathscr{H}^{(s)}_{SPP} = \tilde{g}_{SP_1P_2} S P_1 P_2 . \tag{5}$$

Here again we construct $\tilde{g}_{SP_1P_2}$ from an SU(3)-invariant g_{SPP}, allowing for SU(3) breaking by using the data on the total widths of the scalars. This time $\tilde{g}_{SP_1P_2}$ is symmetric in P_1 and P_2. The coefficients $\tilde{g}_{SP_1P_2}$ are given in terms of g_{SPP} in Table III and the numerical values of g_{S_aPP} ($S_a = \delta', \kappa, \epsilon', S^*$) are given in Table IV. $g_{\delta PP}$ cannot be obtained from the experimental data, and has been calculated using SU(3) symmetry of the scalar nonet.

Now we must construct the weak vertices. CP invariance, Hermiticity, and the SU(4) structure of the weak nonleptonic Hamiltonian [in (1)] leads us to

$$\mathscr{H}^{(w)}_{VPP} = i\mathscr{G}_W \cos^2\theta_C C_{VP_1P_2} V^\mu P_1 \overleftrightarrow{\partial}_\mu P_2 . \tag{6}$$

A term $V^\mu \partial_\mu (P_1P_2)$ is also allowed, but such a term cancels the pole from the propagator (in the narrow-width approximation) and contributes only to the nonpole background. Since we are constructing a pole model for the decays we will ignore this term. The constant $\mathscr{G}_W$ is the usual Fermi constant modified by wave-function overlap terms. As we will confine ourselves to calculating ratios of rates the value of $\mathscr{G}_W$ will not concern us. $C_{VP_1P_2}$ are the CM factors discussed in Sec. II A. They were calculated precisely as in Ref. 1, and are given in Table V. The constant z appearing in Table V was introduced by Cabibbo and Maiani to allow for the difference when the vector is formed from the spectator quark or from a quark-antiquark pair involved in the weak interactions. For the reasons given in Ref. 1 we set $z = 1$ in our numerical calculations.

In a similar way we construct

$$\mathscr{H}^{(w)}_{SPP} = \mathscr{G}_W \cos^2\theta_C T C_{SP_1P_2} S P_1 P_2 . \tag{7}$$

TABLE III. Strong SP_1P_2 coupling constants. $\tilde{g}_{SP_1P_2}$ are as defined by Eq. (5) of text. $\tilde{g}_{SP_1P_2}$ are symmetric in P_1 and P_2, so only coefficients from $m_2 \geq m_1$ are listed. λ is the quadratic ϵ'-S^* mixing angle. The numerical values are calculated using the couplings g_{SPP} of Table IV. S_1^* (ϵ_8') is the pure SU(3) singlet (octet).

S	P_1	P_2	$\tilde{g}_{SP_1P_2}$ (algebraic)	$\tilde{g}_{SP_1P_2}$ (numerical value in GeV)
δ'^+	K^-	K^0	$+\sqrt{2}g_{\delta'PP}$	3.68
δ'^+	π^-	η^0	$+(2/\sqrt{3})g_{\delta'PP}$	3.00
δ'^0	π^0	η^0	$+(2/\sqrt{3})g_{\delta'PP}$	3.00
δ'^0	K^+	K^-	$+(1)g_{\delta'PP}$	2.6
δ'^0	K^0	$\bar{K}^0$	$-(1)g_{\delta'PP}$	−2.6
κ^+	$\bar{K}^0$	π^-	$+\sqrt{2}g_{\kappa PP}$	3.56
κ^+	K^-	π^0	$+(1)g_{\kappa PP}$	2.52
κ^+	K^-	η^0	$-(1/\sqrt{3})g_{\kappa PP}$	−1.46
κ^0	π^+	K^-	$+\sqrt{2}g_{\kappa PP}$	3.56
κ^0	$\bar{K}^0$	π^0	$-(1)g_{\kappa PP}$	−2.52
κ^0	$\bar{K}^0$	η^0	$-(1/\sqrt{3})g_{\kappa PP}$	−1.46
ϵ'	π^+	π^-	$(2/\sqrt{3})g_{\epsilon_8'PP}\cos\lambda+(1/\sqrt{2})g_{S_1^*PP}\sin\lambda$	3.51
ϵ'	π^0	π^0	$(1/\sqrt{3})g_{\epsilon_8'PP}\cos\lambda-(1/2\sqrt{2})g_{S_1^*PP}\sin\lambda$	1.11
ϵ'	K^+	K^-	$-(1/\sqrt{3})g_{\epsilon_8'PP}\cos\lambda+(1/\sqrt{2})g_{S_1^*PP}\sin\lambda$	−0.79
ϵ'	K^0	$\bar{K}^0$	$-(1/\sqrt{3})g_{\epsilon_8'PP}\cos\lambda-(1/\sqrt{2})g_{S_1^*PP}\sin\lambda$	−2.08
ϵ'	η^0	η^0	$-(1/\sqrt{3})g_{\epsilon_8'PP}\cos\lambda-(1/2\sqrt{2})g_{S_1^*PP}\sin\lambda$	−1.76
S^*	K^+	K^-	$+(1/\sqrt{2})g_{S_1^*PP}\cos\lambda+(1/\sqrt{3})g_{\epsilon_8'PP}\sin\lambda$	2.16
S^*	K^0	$\bar{K}^0$	$-(1/\sqrt{2})g_{S_1^*PP}\cos\lambda+(1/\sqrt{3})g_{\epsilon_8'PP}\sin\lambda$	−0.99
S^*	π^-	π^+	$+(1/\sqrt{2})g_{S_1^*PP}\cos\lambda-(2/\sqrt{3})g_{\epsilon_8'PP}\sin\lambda$	0.41
S^*	π^0	π^0	$-(1/2\sqrt{2})g_{S_1^*PP}\cos\lambda-(1/\sqrt{3})g_{\epsilon_8'PP}\sin\lambda$	−1.37
S^*	η^0	η^0	$-(1/2\sqrt{2})g_{S_1^*PP}\cos\lambda+(1/\sqrt{3})g_{\epsilon_8'PP}\sin\lambda$	−0.20

The parameter T, which has dimensions of mass, allows for the difference in the wave-function overlap in the scalar and vector cases. The CM coefficients $C_{SP_1P_2}$ are constructed exactly as before, and are tabulated in Table VI. The parameter r is analogous to z. In our numerical calculation we set $r=1$ for the same reason that we used $z=1$.

TABLE IV. Numerical values of g_{SPP} coupling constants in GeV used in our calculations.

S	g_{SPP}	Source
κ	2.52	experimental
S_1^*	2.41	experimental
ϵ_8'	2.68	experimental
δ'	2.6	theoretical estimate

III. CALCULATIONS AND RESULTS

In our model there are 25 Cabibbo-allowed decay modes of the D and F mesons. Most of these have contributions from more than one pole diagram. The pole diagrams are uniquely identified by their weak vertices (as numbered in Tables V and VI). In Table VII we list these 25 decays, identifying (by the weak vertices) the pole diagrams which contribute to them.

In calculating the diagrams we have introduced finite-width propagators through the replacement

$$\frac{1}{p^2-m^2+i\epsilon} \rightarrow \frac{1}{p^2-m^2+im\Gamma}\ , \tag{8}$$

where m is the resonance mass and Γ is its total width. Integrating over the phase space, the decay

TABLE V. CM vertex factors $C_{VP_cP_3}$ [defined in Eq. (6)] which are required in this paper for VP_cP_3 vertices. The serial number associated with each vertex is used to label the associated pole diagram. In numerical calculations the parameter Z was set to unity (see text).

Serial number	$P_c \to VP_3$	$C_{VP_cP_3}$
1	$D^+ \to \rho^+ \bar{K}^0$	$\sqrt{3}[X_+ + ZX_-]$
2	$\to \bar{K}^{*0} \pi^+$	$\sqrt{3}[ZX_+ + X_-]$
3	$D^0 \to K^{*-} \pi^+$	$Z\sqrt{3}X_+$
4	$\to \rho^+ K^-$	$\sqrt{3}X_+$
5	$\to \bar{K}^{*0} \pi^0$	$\sqrt{3/2}X_-$
6	$\to \rho^0 \bar{K}^0$	$Z\sqrt{3/2}X_-$
7	$\to \bar{K}^{*0} \eta^0$	$(1/\sqrt{2})X_-$
8	$\to \omega \bar{K}^0$	$Z\sqrt{3/2}X_-$
9	$\to \bar{K}^{*0} \eta'$	X_-
10	$F^+ \to \phi \pi^+$	$Z\sqrt{3}X_+$
11	$\to \rho^+ \eta^0$	$\sqrt{2}X_+$
12	$\to \bar{K}^{*0} K^+$	$\sqrt{3}X_-$
13	$\to K^{*+} \bar{K}^0$	$Z\sqrt{3}X_-$
14	$\to \rho^+ \eta'$	$-X_+$

rates may be expressed as quadratic functions of the unknown parameter T,

$$\Gamma(P_c \to P_1 P_2 P_3) = \mathcal{G}_W^2 \cos^4\theta_C (AT^2 + BT + C) , \tag{9}$$

and we tabulate the coefficients A, B, and C in Table VIII.

We quote Kirby *et al.*[25] for experimental data on three-body decay. (There seems to be no subsequent improvement in the quality of this data.[2]) The branching ratios are as follows:

(a) $B(D^0 \to \bar{K}^0 \pi^+ \pi^-) = (3.1 \pm 0.7)\%$,

(b) $B(D^0 \to K^- \pi^+ \pi^0) = (6.7 \pm 2.1)\%$,

(c) $B(D^+ \to K^- \pi^+ \pi^+) = (4.5 \pm 0.8)\%$,

(d) $B(D^+ \to \bar{K}^0 \pi^+ \pi^0) = (15.3 \pm 9.0)\%$.

Taking ratios of branching ratios we have three pieces of experimental information, which turn out to be rather insensitive to the parameter T. From the data we obtain the limit

$$|T| < 2.5 \text{ GeV} . \tag{10}$$

This is a conservative estimate resulting from consideration of the two ratios

$$r_1 = \frac{\Gamma(D^0 \to K^- \pi^+ \pi^0)}{\Gamma(D^0 \to \bar{K}^0 \pi^+ \pi^-)} = 2.16 \pm 0.83 ,$$
$$r_2 = \frac{\Gamma(D^+ \to \bar{K}^0 \pi^+ \pi^0)}{\Gamma(D^+ \to K^- \pi^+ \pi^+)} = 3.4 \pm 2.1 \tag{11}$$

TABLE VI. CM factors $C_{SP_cP_3}$ [defined in Eq. (7)] which are required in this paper. The serial number associated with the vertex is used to label the associated pole diagram. The parameter r is set equal to unity in our numerical calculations. For convenience the mixing-angle (λ) dependent coefficients are also given numerically.

Serial number	$P_c \to PS$	$C_{SP_cP_3}$	$C_{SP_cP_3}$ with numerical value of λ
15	$D^+ \to \bar{K}^0 \delta'^+$	$\sqrt{3}(rX_- + X_+)$	
16	$\to \bar{\kappa}^0 \pi^+$	$\sqrt{3}(X_- + rX_+)$	
17	$D^0 \to \kappa^- \pi^+$	$r\sqrt{3}X_+$	
18	$\to K^- \delta'^+$	$\sqrt{3}X_+$	
19	$\to \bar{K}^0 \delta'^0$	$r\sqrt{3/2}X_-$	
20	$\to \bar{K}^0 \epsilon'$	$r[\sin\lambda + (\cos\lambda)/\sqrt{2}]X_-$	$(1.03)rX_-$
21	$\to \bar{K}^0 S^*$	$r[\cos\lambda - (\sin\lambda)/\sqrt{2}]X_-$	$(0.66)rX_-$
22	$\to \bar{\kappa}^0 \pi^0$	$\sqrt{3/2}X_-$	
23	$\to \bar{\kappa}^0 \eta^0$	$\sqrt{1/2}X_-$	
24	$\to \bar{\kappa}^0 \eta'^0$	X_-	
25	$F^+ \to \bar{\kappa}^0 K^+$	$\sqrt{3}X_-$	
26	$\to \bar{K}^0 \kappa^+$	$r\sqrt{3}X_-$	
27	$\to \pi^+ \epsilon'$	$r(\sqrt{2}\cos\lambda - \sin\lambda)X_+$	$(0.93)rX_+$
28	$\to \pi^+ S^*$	$-r(\sqrt{2}\sin\lambda + \cos\lambda)X_+$	$-(1.46)rX_+$
29	$\to \delta'^+ \eta$	$\sqrt{2}X_+$	
30	$\to \delta'^+ \eta'$	$-X_+$	

TABLE VII. Pole-term contributions to the 25 Cabibbo-favored decay modes of D^+, D^0, and F^+ considered in the paper. The pole terms are labeled by the serial number of the weak vertex occurring in them, according to the numbering in Tables V and VI.

$P_c \to PPP$	Contributions	$P_c \to PPP$	Contributions
$D^+ \to \bar{K}^0 \bar{K}^0 K^+$	1,15	$F^+ \to K^- \pi^+ K^+$	10,12,25,27,28
$\to \bar{K}^0 \pi^+ \pi^0$	1,2,16	$\to \bar{K}^0 \pi^0 K^+$	12,13,25,26
$\to K^- \pi^+ \pi^+$	2,16	$\to \bar{K}^0 \eta^0 K^+$	12,13,11,25,26,29
$\to \bar{K}^0 \pi^+ \eta^0$	2,15,16	$\to \bar{K}^0 K^0 \pi^+$	10,13,26,27,28
		$\to \pi^+ \pi^+ \pi^-$	27,28
$D^0 \to K^- \pi^+ \pi^0$	3,4,5,17,22	$\to \pi^+ \pi^0 \pi^0$	27,28
$\to \bar{K}^0 \pi^- \pi^+$	3,6,17,20,21	$\to \pi^+ \eta^0 \eta^0$	27,28,29
$\to \bar{K}^0 \pi^0 \pi^0$	5,6,20,21,22	$\to K^+ \bar{K}^0 \eta^{0\prime}$	14,30
$\to \bar{K}^0 \pi^0 \eta^0$	5,7,19,22,23	$\to \pi^+ \eta^0 \eta^{0\prime}$	30
$\to K^- \pi^+ \eta^0$	3,7,17,18,23	$\to \eta^0 \pi^+ \pi^0$	11
$\to \bar{K}^0 \pi^0 \eta^{0\prime}$	9,24	$\to \eta^{0\prime} \pi^+ \pi^0$	14
$\to K^- \pi^+ \eta^{0\prime}$	9,24		
$\to \bar{K}^0 \eta^0 \eta^0$	7,20,21,23		
$\to \bar{K}^0 \eta^0 \eta^{0\prime}$	kinematically forbidden		
$K^- \bar{K}^0 K^+$	4,6,18,19,20,21		
$\bar{K}^0 \bar{K}^0 K^0$	6,19,20,21		

TABLE VIII. The numerical constants A, B, and C [defined in Eq. (9)] for the 25 decays considered in this paper.

	$P_c \to P_1 P_2 P_3$ mode	A (GeV^{-1})	B (GeV^0)	C (GeV^1)
1	$F^+ \to \pi^+ \eta^0 \eta^{0\prime}$	1.474×10^{-4}	0	0
2	$F^+ \to \eta^0 \pi^+ \pi^0$	0	0	2.751×10^{-1}
3	$F^+ \to \eta^{0\prime} \pi^+ \pi^0$	0	0	4.635×10^{-2}
4	$F^+ \to \pi^+ \pi^0 \pi^0$	1.988×10^{-2}	0	0
5	$F^+ \to \pi^+ \pi^+ \pi^-$	4.284×10^{-3}	0	0
6	$F^+ \to K^+ \bar{K}^0 \eta^{0\prime}$	2.734×10^{-5}	-5.387×10^{-7}	9.964×10^{-7}
7	$D^0 \to K^- \pi^+ \eta^{0\prime}$	1.673×10^{-6}	$+3.463 \times 10^{-6}$	3.934×10^{-5}
8	$D^0 \to \bar{K}^0 \pi^0 \eta^{0\prime}$	8.343×10^{-7}	$+3.514 \times 10^{-6}$	1.966×10^{-5}
9	$D^+ \to K^- \pi^+ \pi^+$	5.237×10^{-3}	$+2.284 \times 10^{-3}$	1.130×10^{-1}
10	$D^+ \to \bar{K}^0 \bar{K}^0 K^+$	2.324×10^{-3}	-1.105×10^{-5}	1.369×10^{-4}
11	$F^+ \to \pi^+ \eta^0 \eta^0$	3.180×10^{-3}	0	0
12	$D^+ \to \bar{K}^0 \pi^+ \eta^0$	2.045×10^{-3}	-8.108×10^{-4}	8.041×10^{-4}
13	$D^+ \to \bar{K}^0 \pi^+ \pi^0$	2.620×10^{-3}	-2.380×10^{-3}	2.412×10^{-1}
14	$F^+ \to \bar{K}^0 K^+ \pi^0$	1.381×10^{-4}	-8.561×10^{-6}	1.071×10^{-2}
15	$D^0 \to \bar{K}^0 \bar{K}^0 K^0$	5.613×10^{-5}	$+2.901 \times 10^{-8}$	2.513×10^{-6}
16	$D^0 \to \bar{K}^0 \eta^0 \eta^0$	3.882×10^{-6}	$+7.877 \times 10^{-7}$	1.617×10^{-6}
17	$D^0 \to \bar{K}^0 \pi^0 \pi^0$	2.898×10^{-4}	$+9.882 \times 10^{-7}$	2.253×10^{-3}
18	$F^+ \to K^- K^+ \pi^+$	4.239×10^{-3}	$+1.795 \times 10^{-4}$	1.400×10^{-1}
19	$D^0 \to K^- \pi^+ \eta^0$	3.166×10^{-3}	-7.816×10^{-4}	1.987×10^{-3}
20	$D^0 \to \bar{K}^0 \pi^0 \eta^0$	6.469×10^{-5}	$+4.011 \times 10^{-5}$	3.897×10^{-4}
21	$F^+ \to \bar{K}^0 K^0 \pi^+$	2.399×10^{-3}	-3.613×10^{-3}	1.260×10^{-1}
22	$D^0 \to \bar{K}^0 \pi^- \pi^+$	8.039×10^{-3}	$+4.946 \times 10^{-3}$	1.671×10^{-1}
23	$D^0 \to K^- \pi^+ \pi^0$	3.906×10^{-3}	$+8.422 \times 10^{-3}$	3.208×10^{-1}
24	$D^0 \to K^- \bar{K}^0 K^+$	3.359×10^{-3}	-1.014×10^{-4}	2.013×10^{-4}
25	$F^+ \to \bar{K}^0 K^+ \eta^0$	4.614×10^{-3}	$+9.718 \times 10^{-6}$	6.908×10^{-4}

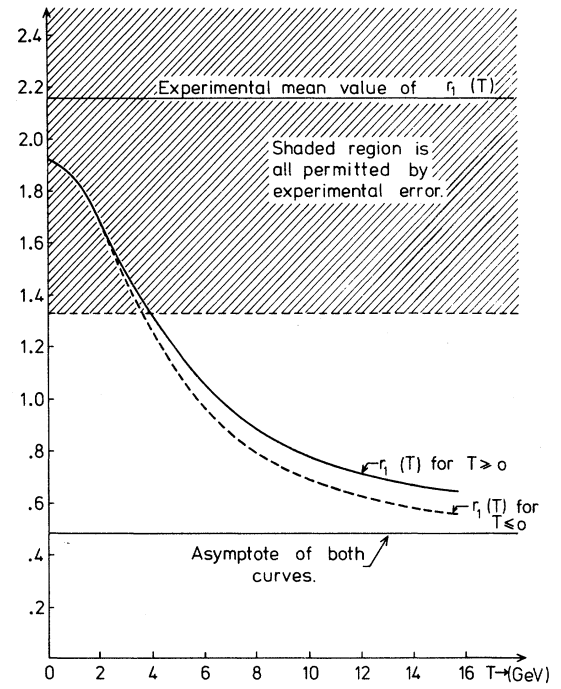

FIG. 5. A plot of $r_1(T)$ compared with experimentally permitted region. (The negative half plane folded onto the positive half plane.)

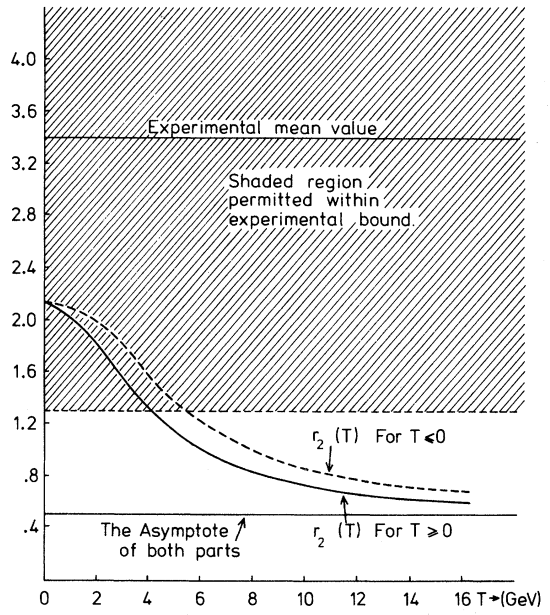

FIG. 6. A plot of $r_2(T)$ compared with experimentally permitted region. (The negative half plane folded onto the positive half plane.)

(experimental values indicated) while from Table VIII our predictions are

$$r_1(T)=\frac{(3.906)T^2+(8.422)T+320.8}{(8.039)T^2+(4.946)T+167.1}\,,$$
$$r_2(T)=\frac{(2.620)T^2+(-2.380)T+241.2}{(5.237)T^2+(2.284)T+113.0}\,. \tag{12}$$

In Figs. 5 and 6 these functions are plotted along with the experimentally permitted domain given in (11). [Note that the left half plane (negative T) has been folded onto the right half plane (positive T) for comparison.] The experimental data would have to be vastly improved in order to determine the sign of T, this explains the modulus signs in (10).

For a representative value of T, $T=0.9$ GeV, we present in Table IX the relative rates of the Cabibbo-allowed modes, in column 1 relative to the largest single three-body mode ($D^0\to K^-\pi^+\pi^0$), and in column 3 relative to the strongest three-body decay mode of the decaying meson. For comparison with the data, in column 4 we use the most accurately experimentally known three-body branching ratio for D^+ and D^0 and our results for $T=0.9$ GeV to predict the branching ratios of the other modes. Because r_1 or r_2 individually yields the bound in (10) one may consider either one of the following as a *prediction* (the other is then viewed as providing the T bound)

$$\text{(b')}\quad B(D^0\to K^-\pi^+\pi^0)=(5.8\pm1.3)\%\,,$$

$$\text{(d')}\quad B(D^+\to \bar{K}^0\pi^+\pi^0)=(9.1\pm1.6)\%$$

which result for $T=0.9$ GeV. Either view is consistent with the data (b) and (d).

To illustrate the sensitivity of our results to T, column 2 of Table IX gives the relative rates for $T=0$, for comparison with the results of column 1. Some of the strongly kinematically suppressed modes are sensitive to T, and perhaps it is best determined from $B(F^+\to\pi^+\pi^0\pi^0)/B(F^+\to K^-K^+\pi^+)$ as the denominator is very weakly dependent on T while the numerator is very strongly dependent on T.

To compare relative rates of D^+ and D^0 decays we need the total lifetimes of particles. We can turn this comparison around, using Table IX and the data to predict the lifetime ratio through

$$R=\frac{\tau^+}{\tau^0}=\left[\frac{B(D^+\to X)}{B(D^0\to Y)}\right]_{\text{exp}}\left[\frac{\Gamma(D^0\to X)}{\Gamma(D^+\to Y)}\right]_{\text{calculated}}\,. \tag{13}$$

TABLE IX. Relative rates and branching ratios of Cabibbo-favored three-body decay modes of charmed mesons. Relative rates 1 are relative to $\Gamma(D^0\to K^-\pi^+\pi^0)$ while relative rates 2 are relative to the largest mode of the decaying particle. Branching ratios are obtained using those branching ratios marked * as input.

Mode	Relative rate 1 ($T=0.9$ GeV)	Relative rate 1 ($T=0$ GeV)	Relative rate 2 ($T=0.9$ GeV)	Branching ratios
$F^+\to\eta^0\pi^+\pi^0$	8.30×10^{-1}	8.58×10^{-1}	1	
$\to K^-K^+\pi^+$	4.33×10^{-1}	4.36×10^{-1}	5.22×10^{-1}	
$\to\bar{K}^0K^0\pi^+$	3.76×10^{-1}	3.93×10^{-1}	4.53×10^{-1}	
$\to\eta'\pi^+\pi^0$	1.40×10^{-1}	1.45×10^{-1}	1.69×10^{-1}	
$\to\pi^+\pi^0\pi^0$	4.86×10^{-2}	0	5.85×10^{-2}	
$\to\bar{K}^0K^+\pi^0$	3.26×10^{-2}	3.34×10^{-2}	3.93×10^{-2}	
$\to\bar{K}^0K^+\eta^0$	1.34×10^{-2}	2.15×10^{-3}	1.61×10^{-2}	
$\to\pi^+\pi^+\pi^-$	1.05×10^{-2}	0	1.26×10^{-2}	
$\to\pi^+\eta^0\eta^0$	7.77×10^{-3}	0	9.36×10^{-3}	
$\to\pi^+\eta^0\eta'$	3.60×10^{-4}	0	4.34×10^{-4}	
$\to K^+\bar{K}^0\eta'$	6.83×10^{-5}	3.11×10^{-6}	8.24×10^{-5}	
$D^+\to\bar{K}^0\pi^+\pi^0$	7.27×10^{-1}	7.52×10^{-1}	1	$(9.1\pm1.6)\%$
$\to K^-\pi^+\pi^+$	3.60×10^{-1}	3.52×10^{-1}	4.95×10^{-1}	$(4.5\pm0.8)\%$*
$\to\bar{K}^0\bar{K}^0K^+$	6.06×10^{-3}	4.27×10^{-4}	8.33×10^{-3}	$(7.6\pm1.3)\times10^{-2}\%$
$\to\bar{K}^0\pi^+\eta^0$	5.22×10^{-3}	2.51×10^{-3}	7.18×10^{-3}	$(6.5\pm1.1)\times10^{-2}\%$
$D^0\to K^-\pi^+\pi^0$	1	1	1	$(5.8\pm1.3)\%$
$\to\bar{K}^0\pi^-\pi^+$	5.37×10^{-1}	5.21×10^{-1}	5.37×10^{-1}	$(3.1\pm0.7)\%$*
$\to K^-\pi^+\eta^0$	1.16×10^{-2}	6.19×10^{-3}	1.16×10^{-2}	$(6.7\pm1.5)\times10^{-2}\%$
$\to K^-\bar{K}^0K^+$	8.54×10^{-3}	6.28×10^{-4}	8.54×10^{-3}	$(5.0\pm1.1)\times10^{-2}\%$
$\to\bar{K}^0\pi^0\pi^0$	7.51×10^{-3}	7.02×10^{-3}	7.51×10^{-3}	$(4.4\pm1.0)\times10^{-2}\%$
$\to\bar{K}^0\pi^0\eta^0$	1.44×10^{-3}	1.22×10^{-3}	1.44×10^{-3}	$(8.4\pm1.9)\times10^{-3}\%$
$\to\bar{K}^0\bar{K}^0K^0$	1.45×10^{-4}	7.83×10^{-6}	1.45×10^{-4}	$(8.4\pm1.9)\times10^{-4}\%$
$\to K^-\pi^+\eta'$	1.32×10^{-4}	1.23×10^{-4}	1.32×10^{-4}	$(7.7\pm1.7)\times10^{-4}\%$
$\bar{K}^0\pi^0\eta'$	7.09×10^{-5}	6.13×10^{-5}	7.09×10^{-5}	$(4.1\pm0.9)\times10^{-4}\%$
$\bar{K}^0\eta^0\eta^0$	1.65×10^{-5}	5.04×10^{-6}	1.65×10^{-5}	$(9.6\pm2.1)\times10^{-5}\%$

If we use the experimental facts that

$$\frac{B(D^+\to K^-\pi^+\pi^+)}{B(D^0\to\bar{K}^0\pi^+\pi^-)}=1.45\pm0.42 \tag{14}$$

and

$$\frac{B(D^+\to\bar{K}^0\pi^+\pi^-)}{B(D^0\to K^-\pi^+\pi^0)}=2.28\pm1.52\ ,$$

then along with Table VIII this gives two determinations of R,

$$R_1(T)=\left[\frac{T^2(8.039)+T(4.946)+167.1}{T^2(5.237)+T(2.284)+113.0}\right]\times(1.45\pm0.42)\ ,$$
$$R_2(T)=\left[\frac{T^2(3.906)+T(8.422)+320.8}{T^2(2.620)+T(-2.380)+241.2}\right]\times(2.28\pm1.52)\ . \tag{15}$$

These functions are plotted in Fig. 7 for $|T|<2.5$ GeV. They vary very slowly with T. Considering the experimental errors, R_1 and R_2 are quite consistent with each other.

We quote R values at $T=0.9$ GeV and find

$$R_1(0.9)=2.16\pm0.63\ ,$$
$$R_2(0.9)=3.13\pm2.09\ . \tag{16}$$

A weighted mean gives

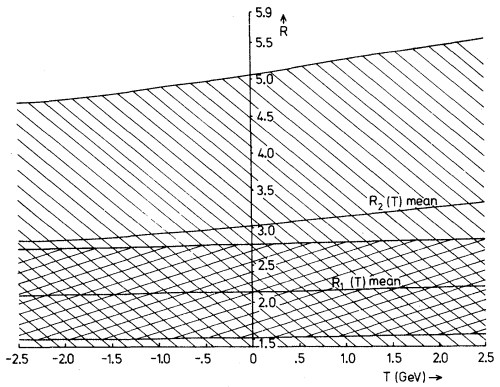

FIG. 7. The functions $R_1(T)$ and $R_2(T)$ with error regions, plotted for $T \leq 2.5$ GeV.

$$R\ (T=0.9\ \text{GeV}) = 2.24 \pm 0.60\ . \tag{17}$$

This result is quite consistent with datum (1′). We emphasize that our model is naturally compatible with unequal D^+ and D^0 lifetimes, whatever mechanism is responsible for the effect. No contrivance was necessary to obtain (17).

In fact independent of T, R_1 implies

$$1.51 \leq R \leq 2.90 \tag{18}$$

which is only a slightly broader domain than (17) itself.

IV. CONCLUSIONS

We have shown how the spectator model may implicate a pole model of three-body decays of the charmed D and F mesons. This model is consistent with the available data on the relative rates of three-body decays of D^0 and D^+, and with the present value of the lifetime ratio.

That a pole model works is not surprising in view of the Dalitz-plot analysis of the decays.[2] The $D^0 \to \bar{K}^0 \pi^+ \pi^-$ decay mode is dominated by the $K^{*-}\pi^+$ contribution ($70^{+14}_{-16}\%$), the $\bar{K}^0\rho^0$ contribution is small ($2^{+9}_{-2}\%$), and the "nonresonant" background is $30^{+17}_{-14}\%$. $D^0 \to K^-\pi^+\pi^0$ is dominated by the ρ^+K^- contribution ($85^{+10}_{-15}\%$), with small contributions from $\bar{K}^{*0}\pi^0$ ($11^{+16}_{-11}\%$) and $K^{*-}\pi^+$ ($7^{+8}_{-4}\%$) and the "nonresonant" background ($6^{+6}_{-0}\%$). The Dalitz plot for $D^+ \to K^-\pi^+\pi^+$ is neither uniformly populated nor dominated by the $\bar{K}^{*0}\pi^+$ mode, for which an upper limit of 39% is estimated. No scalar meson enhancements have been seen in the analysis, but these resonances are very broad and provide a small contribution to the observed decays. They should not be expected to be visible experimentally until much higher statistics are available.

TABLE X. Branching ratios predicted by the model for observed $D^0 \to VP$ decays, compared with experimental values. The rate marked with an asterisk was used as input in the calculation.

Decay mode	Predicted branching ratio (%)	Observed branching ratio (%)
$D^0 \to K^{*-}\pi^+$		$3.3 \pm 1.2^*$
$\to K^-\rho^+$	3.7 ± 1.4	$7.2^{+2.9}_{-3.0}$
$\to \bar{K}^0\rho^0$	0.09 ± 0.03	$0.1^{+0.3}_{-0.1}$
$\to \bar{K}^{*0}\pi^0$	0.08 ± 0.03	$1.4^{+2.1}_{-1.4}$

For our model to be consistent, it should predict the relative branching ratios for charmed-meson decay into vector and pseudoscalar mesons. The observed branching ratios are given in Table X and are compared to the predictions of our model. The agreement is acceptable, and provides further support for the model. Not only do we predict overall three-body branching ratios well, but also the constituent vector-pseudoscalar branching ratios.

In conclusion we find that our spectator-based model is in good agreement with the data on three-body decays of charmed mesons—the inconsistencies seen in the $K\pi$ decays of D mesons do not propagate into the three-body sector.

ACKNOWLEDGMENTS

B.H.J. McKellar wishes to thank the T5 group for their hospitality at Los Alamos, and the Australian Educational Foundation for the award of a Fullbright Travel Grant.

*Permanent address.

[1]N. Cabibbo and L. Maiani, Phys. Lett. 73B, 418 (1978).

[2]A. J. Lankford, in *High Energy Physics—1980,* proceedings of the XXth International Conference, Madison, Wisconsin, edited by L. Durand and L. G. Pondrom (AIP, New York, 1981), p. 373; see also Fermilab Experiment 531 Collaboration (N.R. Stanton *et al.*), in *Neutrino 81,* proceedings of the International Conference on Neutrino Physics and Astrophysics,

Maui, Hawaii, edited by R. J. Cence, E. Ma, and A. Roberts (University of Hawaii, High Energy Physics Group, Honolulu, 1981), p. 491.

[3]J. P. Leveille, Report No. UM HE 81-18, 1981 (unpublished).

[4]S. Pakvasa, in *High Energy Physics—1980* (Ref. 2), p. 1164.

[5]V. Barger, J. P. Leveille, and P. M. Stevenson, Phys. Rev. Lett. 44, 226 (1980); Report No. SLAC-Pub-2596, 1980 (unpublished); C. Schmid, Zurich report, 1981 (unpublished); M. Bovin and C. Schmid, Zurich report, 1980 (unpublished); X. Y. Pham, Acta Phys. Pol. B11, 735 (1980); K. Terasaki, Prog. Theor. Phys. 66, 988 (1981).

[6]M. Bander, D. Silverman, and A. Soni, Phys. Rev. Lett. 44, 4 (1980); 44, 962 (1980); H. Fritzsch and P. Minkowski, Phys. Lett. 90B, 455 (1980); B. Guberina, D. Tadić, and J. Trampetić, Zagreb report, 1981 (unpublished).

[7]W. Bernreuther, O. Nachtman, and B. Stech, Z. Phys. C 4, 257 (1980); H. Fritzsch and P. Minkowski, Phys. Lett. 90B, 455 (1980); K. Shizuya, *ibid.* 100B, 79 (1981).

[8]However, H. C. Lee and Q. H. Kim, Phys. Rev. D 25, 178 (1982), have shown that Gqq process is not competitive with the spectator process.

[9]B. Guberina, S. Nussinov, R. D. Peccei, and R. Ruckl, Phys. Lett. 89B, 111 (1979); G. Eilam, B. H. J. McKellar, and M. D. Scadron, Oregon Report No. OITS-168, 1981 (unpublished); L. S. Dulyan and A. Yu. Khodjamirian, Yerevan Report No. EΦ*n*-4I0(17)-80, 1980 (unpublished).

[10]H. J. Lipkin, Phys. Rev. Lett. 44, 710 (1980); A. N. Kamal and E. D. Cooper, Z. Phys. C 8, 67 (1981).

[11]Note however that the final-state interaction can link the $K\pi$ and $K\pi\pi\pi$ channels and must be treated in a multichannel formulation. But first we need a model for the $D\to K\pi\pi\pi$ process, which has a large branching ratio. If final-state interactions are important, the situation is likely to be much more complicated than described in Ref. 10.

[12]T. Tanuma, S. Oneda, and K. Terasaki, Phys. Lett. 110B, 260 (1982); D. G. Sutherland, *ibid.* 90B, 173 (1980); G. L. Kane, Report No. SLAC-Pub-2326, 1979 (unpublished); Y. Igarashi, S. Kitakado, and M. Kuroda, Phys. Lett. 93B, 125 (1980).

[13]K. Terasaki, Prog. Theor. Phys. 66, 98 (1981).

[14]A. Yu. Khodjamirian, Yerevan Report No. EΦ*n*-346(4)-79, 1979 (unpublished).

[15]E. Sezgin, Phys. Rev. D 19, 2142 (1979).

[16]Y. Hara, Prog. Theor. Phys. 61, 1738 (1979).

[17]S. P. Rosen, Phys. Lett. 89B, 246 (1980).

[18]M. D. Scadron and L. R. Thebaud, Phys. Rev. D 8, 2190 (1973).

[19]A. Le Yaouanc, O. Pine, J. C. Raynal, and L. Oliver, Nucl. Phys. B149, 321 (1979).

[20]L. S. Dulyan and A. Yu. Khodjamirian, Yerevan Report No. EΦ*n*-UI0(17)-80, 1980 (unpublished); A. Yu. Khodjamirian, Yad. Fiz. 30, 824 (1979) [Sov. J. Nucl. Phys. 30, 425 (1979)].

[21]In R. D. C. Miller and B. H. J. McKellar, J. Phys. G 8, L1 (1982) and University of Melbourne Report No. UM-P-81/56 (unpublished), we have suggested that $f_+=0.77$, $f_-=1.68$, leading to $X_+=1.07$, $X_-=0.05$, is to be preferred. But to emphasize that our results are those of the usual spectator model we have presented the numerical results for the conventional choice of parameters of Eq. (2).

[22]P. Estabrooks, Phys. Rev. D 19, 2678 (1979).

[23]R. J. Cashmore, in *Proceedings of the 19th International Conference on High Energy Physics, Tokyo, 1978,* edited by S. Homma, M. Kawaguchi, and H. Miyazawa (Phys. Soc. of Japan, Tokyo, 1979), p. 811.

[24]In making our estimates of the contribution of D^* and F^* poles we noted that Eq. (4) holds for charmed particles if we impose SU(4) flavor symmetry. Since total widths of D^* and F^* are unknown in this case we used SU(4) symmetry to obtain the necessary coupling constants.

[25]J. Kirkby *et al.*, in *Proceedings of the 1979 International Symposium on Lepton and Photon Interactions at High Energies, Fermilab,* edited by T. B. W. Kirk and H. D. I. Abarbanel (Fermilab, Batavia, Illinois, 1980), p. 107.